15

Flexible multibody systems: preliminaries

Multibody systems are characterized by two distinguishing features: system components undergo finite relative rotations and these components are connected by mechanical joints that impose restrictions on their relative motion. Broadly speaking, multibody systems can be divided into three categories, rigid multibody systems, linearly elastic multibody systems, and nonlinearly elastic multibody systems. This classification and its implication on modeling techniques for multibody systems are discussed in section 15.1.

Section 15.2 presents a review of the basic equations of three-dimensional, linear elastodynamics. Geometrically nonlinear problems are characterized by nonlinear strain-displacement relationships, which are the subject of section 15.3. In section 15.5, special attention is devoted to the formulation of problems where structures undergo arbitrarily large displacements and rotations although strain components are assumed to remain small at all points of the structure.

15.1 Classification of multibody systems

Multibody systems can be divided into three categories, rigid multibody systems, linearly elastic multibody systems, and nonlinearly elastic multibody systems. Systems of the first category involves rigid bodies only, but those of the latter two categories comprise both rigid and flexible bodies. Section 12.5.1 introduced the concept of floating frame of reference in which the total motion of flexible bodies is broken into two parts: rigid body motions represented by the motion of the floating frame of reference and superimposed elastic motions. By definition, rigid body motions generate no strains. The elastic motions typically consist of displacement and rotation fields, which generate an associated strain field, denoted $\underline{\epsilon}$. For rigid multibody system, the strain field vanishes in all bodies, *i.e.*, $\underline{\epsilon} = 0$ in each body. The distinction between linearly and nonlinearly elastic multibody systems stems from the characteristics of the strain field.

The characteristics of the three types of multibody systems are as follows.

O. A. Bauchau, *Flexible Multibody Dynamics,*
DOI 10.1007/978-94-007-0335-3_15

1. *Rigid multibody systems* consist of an assemblage of rigid bodies connected together through mechanical joints and in arbitrary motion with respect to each other. Although all bodies are rigid, *i.e.*, $\underline{\epsilon} = 0$ in each body, lumped elastic components, also called *flexible joints*, *bushing elements* or *force elements*, could be placed between two components of the system to represent localized elasticity. These flexible joints exhibit arbitrary constitutive behavior.
2. *Linearly elastic multibody systems* consist of an assemblage of both elastic and rigid bodies connected together through mechanical joints and in arbitrary motion with respect to each other. For linearly elastic multibody systems, it is assumed that the strain-displacement relationships remain linear and that strains components remain very small at all times, *i.e.*, $\underline{\epsilon} \ll 1$ for all elastic bodies. Efficient analysis techniques for this type of problems typically rely on modal expansions of the elastic displacement field.
3. *Nonlinearly elastic multibody systems* consist of an assemblage of both elastic and rigid bodies connected together through mechanical joints and in arbitrary motion with respect to each other. For the elastic bodies, the strain-displacement relationships become nonlinear, or the strain components become large, or both. Nonlinear strain-displacement relationships characterize *geometrically nonlinear problems*, *i.e.*, problems involving large elastic displacements, or rotations, or both. When strain components become large, nonlinear material constitutive laws must be used, a characteristic of *materially nonlinear problems*. For nonlinearly elastic multibody systems the accuracy and reliability of modal expansion of the elastic displacement field become questionable.

Because the overall motions of all bodies of a multibody system are large and because the relative motions between the system's various components are also large, multibody system dynamics is an inherently nonlinear problem. The qualifiers "linearly" and "nonlinearly elastic" used in the classification above specifically refer to the elastic behavior of the bodies. The modeling of linearly elastic multibody systems leads to nonlinear dynamical equations of motion, although the representation of the elastic behavior of the bodies could be largely linearized.

15.1.1 Linearly and nonlinearly elastic multibody systems

The demarcation between linearly and nonlinearly elastic multibody systems is sometimes blurry. Consider, for instance, the problem of a helicopter rotor blade. As the blade rotates, elastic displacements and rotations remain very small, and the blade is designed to undergo small strains at all time to ensure safety of flight and guarantee structural fatigue life. This problem seems to fall into the category of linearly elastic multibody systems.

Due to the high angular speed of the rotor, however, large centrifugal forces appear in the blade, leading to considerable centrifugal stiffening of the blade and nonlinear coupling between its two bending and torsional deformations. To accurately capture these effects, nonlinear strain-displacement relationships must be used, although linear constitutive laws adequately represent material behavior. These geo-

metric nonlinearities squarely put the helicopter rotor blade problem into the category of nonlinearly elastic multibody systems.

Because wind turbine blades rotate at a much lower angular speed and are far stiffer than helicopter rotor blades, assuming wind turbines to be linearly elastic multibody systems often leads to reliable predictions. On the other hand, efforts to design ever increasingly efficient turbines call for ever increasing rotor diameters. It is possible that future generation turbines will become large enough to operate in the geometrically nonlinear regime, requiring the use of formulations capable of dealing with nonlinearly elastic multibody systems to predict accurately the dynamic response of such highly flexible machines.

The distinction between linearly and nonlinearly elastic systems is further complicated by the fact that both linearly and nonlinearly elastic components could appear simultaneously in a given multibody system. For instance, the modeling of a complete helicopter in flight calls for the coupled simulation of the rotor and fuselage. As explained above, the rotor problem is inherently nonlinear, but it is reasonable to assume that the fuselage behaves in a linearly elastic manner, even during large angle maneuvers. For such problems, different formulations could be used to model the rotor and fuselage that reflect the distinctly different behavior of these two components. Similar remarks could be made concerning wind turbines. Whereas the rotor blades could be treated as linearly or nonlinearly elastic bodies depending on the magnitude of the elastic motions, it seems reasonable to assume the supporting tower to behave in a linearly elastic manner.

The remaining chapters of this book focus on nonlinearly elastic multibody systems. As discussed in section 12.5.1, one of the most common approaches to the modeling of linearly elastic multibody systems is based on the concept of floating frames of reference [162] and the component mode synthesis based methods described in section 12.5.2 are then used to approximate the elastic displacement field. For nonlinearly elastic multibody systems the accuracy and reliability of these approaches become questionable for the reasons detailed in the next section.

15.1.2 Shortcomings of modal analysis applied to nonlinear systems

The natural vibration modes of a structure are the eigenfunctions of the system's equations of motion linearized about one of its equilibrium configurations. Therefore, these modes characterize the dynamic behavior of small perturbations about an equilibrium configuration of the system. Clearly, natural vibration modes are inherently linearized quantities that provide no information about the nonlinear behavior of the system.

Consider a simple cantilevered beam under transverse, time-dependent loading. The beam's mode shapes computed with respect to its unloaded configuration include the familiar bending, axial, and torsional modes of vibration, which are derived in numerous structural vibration textbooks such as those of Timoshenko and Young [273] or Meirovitch [183]. If the beam is subjected to a tip transverse load that generates small transverse deflections of the beam, a modal expansion in terms

of transverse bending modes will accurately predict the dynamic behavior of the system, even when using a small number of modes. Of course, resonance conditions should be avoided as large deflections would result. Furthermore, all the modes associated with natural frequencies of magnitude comparable to that of the excitation frequency should be included in the modal expansion.

Modal analysis is a natural approach to reducing the number of degrees of freedom involved in structural dynamics problems, and has the added advantage of involving degrees of freedom that have a direct physical meaning. Modal analysis can be viewed as a two step process.

In the first step of the process, a change of variables is performed by projecting the equations of motion expressed in term of physical variables to the modal domain. For a simple cantilevered beam problem, the physical variables would typically consist of the displacement and rotation components at discrete nodes along the beam. The modal variables are the amplitudes of excitation of the beam's eigenmodes. If all the modes of the structure are used, this change of variable is a purely mathematical operation that involves no approximations.

In the second step of the process, modal truncation is performed. Based on physical arguments, a small subset of all the eigenmodes of the structure is retained. For linear systems, modal truncation is a simple operation: modes associated with frequencies far higher than the excitation frequencies are simply eliminated from the modal basis because their contribution to structural response is negligible.

This assumption yields the major advantages of modal analysis. First, a dramatic reduction in the number of degrees of freedom is achieved, leading to considerable computational savings. For complex structures, thousands or even hundreds of thousands of degrees of freedom might be involved in a detailed finite element model, whereas ten or fifteen modes only could be sufficient to capture accurately the overall dynamic behavior of the structure.

Second, because high frequency modes have been eliminated, larger time step sizes can be used to integrate the system's equations of motion, leading to additional computational savings. Finally, the modal degrees of freedom are easily interpreted in a physical manner. For instance, if a structure responds "mainly in its second bending mode," or "primarily in its first torsion mode," it is easy to visualize the overall deformation of even very complex structure.

Projection of the equations of motion into the modal domain is a purely mathematical step that does not involve any approximation. Modal truncation is an assumption. Indeed, when applied to linear systems, the projection of the equations of motion to the modal space decouples the governing equations. In the modal space, even the most complex structures can be viewed as a superposition of linear, single degree of freedom oscillators. The elimination of specific modes to obtain a reduced modal basis is based on the well known properties of these oscillators.

When applied to nonlinear structures, the first step of the modal analysis process is also the projection of the equations of motion onto the modal domain. As was the case for linear structures, no assumption is involved here. Modal truncation, however is fraught with difficulties. For nonlinear problems, the equations of motion projected in the modal space are still nonlinear and in general, do not decouple. The

nonlinear system cannot be viewed as the superposition of linear, single degree of freedom oscillators, nor can it be viewed as the superposition of nonlinear oscillators. Consequently, the physical arguments invoked to eliminate specific modes from the modal basis no longer apply, or become more tenuous.

To illustrate the problems encountered by modal analysis applied to nonlinear structures, consider the simply supported beam depicted in fig. 15.1. The beam is subjected to time-dependent loading, $p_2(x_1, t)$, and features a large axial stiffness. For case (a), the end points of the beam cannot move axially. In contrast, axial displacements are allowed at point **T** for case (b). For case (a), large transverse displacements of the beam generate axial deformations, which in turn, cause large axial forces to appear due to the beam's high axial stiffness. As the magnitude of the transverse displacements increases, a considerable stiffening of the system is observed, leading to pronounced nonlinear behavior. This phenomenon is much less severe for case (b) because the beam is free to move axially at point **T**.

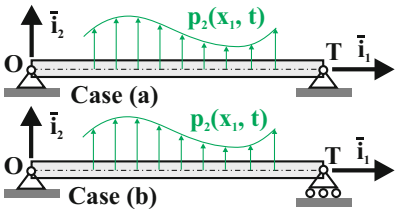

Fig. 15.1. Simply supported beam with different end conditions.

To simplify the discussion, the problems depicted in fig. 15.1 are limited to the planar case where all displacements take place in plane $(\bar{\imath}_1, \bar{\imath}_2)$. The beam's natural vibration modes about its unloaded configuration are easily obtained and consist of transverse bending and axial modes. Because they are linearized quantities, the bending modes involve transverse displacement components only. Note that the beam's bending modes are identical for cases (a) and (b), although its axial modes differ.

If small, time-dependent transverse loads are applied to the beam, modal analysis using a modal basis consisting of a few bending modes yields accurate predictions of the dynamic response of the system. In the linear range, axial modes are not excited and need not be present in the modal basis. The solutions for cases (a) and (b) are identical in the linear range, a feature that is correctly reproduced by the modal solution because the axial displacement boundary condition is not reflected in the modal basis. The modal basis does not "feel" the difference between cases (a) and (b).

Next, larger transverse loads are applied to the beam, which now responds in the nonlinear range. If bending modes only are used in the modal approximation, the beam's dynamic response is no longer predicted accurately. The situation is somewhat improved by adding axial vibration modes, but a large number of these modes is required to obtained a good solution.

The reason for this behavior is twofold. First, because the beam's axial displacement field is not captured accurately by the modal approximation, errors are to be expect in the estimation of the axial strain field. Due to the beam's large axial stiffness, small errors in the axial strain field lead to a grossly erroneous axial force field and the nonlinear stiffening effects it induces are poorly captured by the modal analysis. Clearly, the foreshortening of the blade, an inherent part of its nonlinear response, must be modeled precisely to predict accurately the beam's nonlinear response.

Second, the blade's axial displacement field is primarily due to foreshortening (a purely kinematic, nonlinear phenomenon), whereas axial vibration modes characterize true axial vibration (a purely vibratory, linear phenomenon). In other words, modal analysis attempts to "synthesize" a nonlinear kinematic mode shape as a superposition of linear vibratory modes. Because these two phenomena are not physically related, accurate predictions should hardly be expect from this superposition.

Thus far, the discussion has focussed on nonlinear foreshortening effects in a simple planar problem. The above arguments, however, also apply to other kinematic nonlinearities found in three-dimensional problems. For instance, transverse deflections due to transverse loads applied to the beam in two orthogonal directions create a torsional moment, thereby coupling bending and torsion responses.

When applied to nonlinear problems, convergence and accuracy of modal analysis are not guaranteed. To improve the situation, it seems natural to investigate the selection of alternative mode shapes that contain information about the nonlinear behavior of the structure. Several concepts have been proposed to improve the quality of the modal basis when dealing with nonlinear problems.

The conceptually simplest method it to recalculate a new set of natural vibration modes once the deformations of the blade become significant [274]. Due to the large relative motions between the components of multibody systems, the equilibrium configuration of the system is time-dependent, and hence, the modal basis is itself time-dependent. Although this approach might give good results, it does so at a tremendous computational costs, because the modal basis must now be updated during the response calculation, and the modal reduction scheme must be repeated at each update.

Another approach is to include in the modal basis natural vibration modes about different equilibrium configurations of the structure. This method is attractive because the evaluation of the various equilibrium configurations and associated modal bases only require a modest increase in computational costs. In some cases, this method appears to give accurate results, as documented by Nickell [274].

The concept of perturbation modes was introduced by Thompson and Walker [275] to study the nonlinear behavior of beam structures. The authors demonstrated improved accuracy compared with classical modal analysis based on natural vibration modes. The same concept was later refined by Noor *et al*. [276, 277] for the nonlinear static analysis of beam and shell structures in conjunction with the finite element method. Bauchau and Guernsey [278] also used these concepts for the analysis of helicopter rotors.

Mixed finite element formulations have also been developed to improve the accuracy and reliability of modal methods. Ruzicka and Hodges [279, 280] have demonstrated applications of this method to rotorcraft problems.

While the various approaches described in the previous paragraphs are capable of extending the range of validity of modal methods, they also present many drawbacks. First, they require extensive numerical developments and more often that not, the simplicity of modal analysis is lost. Second, they are based of formulations that are not widely available. For instance, commercial finite element codes are rarely based on mixed formulations. Finally, different approaches are required to deal with

different problem, *i.e.*, these methods are not general purpose methods that can be used reliably for general multibody systems.

15.1.3 Finite element based modeling of flexible multibody systems

Multibody dynamics analysis was originally developed as a tool for modeling rigid multibody systems with simple tree-like topologies, but has considerably evolved to the point where it can handle linearly and nonlinearly elastic multibody systems with arbitrary topologies. It is now used widely as a fundamental design tool in many areas of engineering.

In the automotive industry, for instance, multibody dynamics analysis is used routinely for optimizing vehicle ride qualities, a complex multidisciplinary task that involves the simulation of many different sub-components. Modern multibody codes can deal with complex mechanisms of arbitrary topologies including sensors, actuators, and controls, are interfaced with CAD solid modeling programs that allow to import directly the problem geometry, and have sophisticated graphics, animation, and post-processing features [38, 39].

The success of multibody dynamics analysis tools stems from their versatility: a given mechanism can be modeled by an idealization process that identifies the mechanical components from within a large library of elements implemented in the code. Each element provides a basic functional building block, for example, a rigid or flexible member, a revolute joint, or a motor. Assembling the various elements, it is then possible to construct a mathematical description of the mechanism with the required level of accuracy.

The modeling of linearly elastic multibody systems relies predominantly on the floating frame of reference approach discussed in section 12.5.1, in which the elastic displacement field is approximated using modal expansion techniques. In the last two decades, new approaches have emerged that bypass the need for the floating frame of reference and eliminate modal expansions. These approaches are closely related to the finite element method which they effectively generalize to enable the treatment of multibody systems.

In the finite element method, the solution domain is first divided into a finite number of sub-domains called *finite elements*. Within each element, the solution is then approximated by a small number of continuous functions, based on the value of these functions at discrete points, often called *nodes*, associated with the element. The main advantage of this two-step approximation process is that many aspects of the solution procedure can be carried out at the element level, *i.e.*, by considering one single element at a time, independently of all others.

The continuity of the solution across elements is guaranteed by the fact that neighboring elements share common nodes, *i.e.*, share common degrees of freedom. This aspect of the formulation is key to ensuring the continuity of the displacement field over the entire system, an indispensable requirement for displacement based finite element formulations.

Consider a beam connected at one of its end points to a revolute joint. Complete definition of the beam requires geometric data: typically, a local frame is used to

define the beam's cross-sectional plane and its physical mass and stiffness properties are given with respect to this local frame. Similarly, definition of the revolute joint also requires geometric data: typically, a local frame is used to define the plane of the joint and the unit vector about which relative rotation is allowed, see fig. 10.14. These local frames are independent of each other and are used solely by the elements for which they are defined.

In contrast, the components of the displacement and rotation vectors at the connection point between the beam and revolute joint must be uniquely defined. If the displacement components are resolved in the local frame of the beam element, the revolute joint will not be able to interpret these components properly because they are resolved in a local frame whose orientation it does not know. Vice versa, if the displacement components are resolved in the local frame of the revolute joint, the beam will not be able to interpret these components adequately because they are resolved in a local frame whose orientation it does not know.

To resolve this conflict, all nodal displacement and rotation components must be defined in a common frame, which is conveniently selected to be the *inertial frame of reference*. Because the components of multibody systems typically undergo large displacements and rotations, these inertial, or absolute, displacement and rotation components must be treated rigorously as large displacement and rotation components. Consequently, all the elements of the multibody system must be able to handle arbitrarily large displacements and rotations exactly. This is why these elements are sometimes called "geometrically exact elements," although the term "kinematically exact elements" would be more appropriate.

Finite element based modeling of flexible multibody systems makes use of a library of elements consisting of *structural elements* and *joint elements*. Structural elements, such as cables, membranes, beams, plates, shells, or three-dimensional elements are similar to the corresponding elements found in all finite element packages. The geometrically exact formulations of cables, beams, and plates and shells are presented in sections 16.2, 16.3, and 16.4, respectively. The dynamic equations of equilibrium of these elements are written in an absolute Cartesian frame.

Joint elements characterize multibody systems and are absent from most finite element codes. In typical multibody formulations, joints are modeled as idealized components, *i.e.*, joints are not modeled *per se*. Rather, the effects of joints are represented by the kinematic constraints they impose on the components they are connected to. For instance, section 10.6 details the constraints associated with the lower pair joints, which are enforced via Lagrange's multiplier technique.

The assembly of the equations of motion of both structural and joint elements leads to systems of equations that are highly sparse, although not of minimal size, a characteristic of the approach pioneered by Orlandea *et al.* [77]. Because it is an extension of the finite element method to multibody systems, algorithms such as sparse solvers, assembly procedures, and data structures developed for finite element analysis are directly applicable to finite element based modeling of flexible multibody systems.

This approach can readily treat configurations of arbitrarily complex topologies through the assembly of basic components chosen from an extensive library of struc-

tural and joint elements. In fact, this concept is at the heart of the finite element method which has enjoyed, for this very reason, an explosive growth in the last few decades. This analysis approach leads to new comprehensive simulation tools that are modular and expandable. Modularity implies that all the basic building blocks can be validated independently, easing the more challenging task of validating complete simulation procedures. Because they are applicable to configurations with arbitrary topologies, including those not yet foreseen, such simulation tools will enjoy a longer life span, a critical requirement for any complex software tool.

Example 15.1. Modeling helicopter rotors with flexible multibody dynamics
Historically, the classical approach to rotor dynamics modeling has relied on modal reduction approaches, as pioneered by Houbolt and Brooks [281]. Typical models were limited to single articulated blades connected to an inertial point and the control chain was ignored. The blade's equations of motion were written in the rotating system, and ordering schemes were used to decrease the number of nonlinear terms appearing in the modal expansion [282].

In time, more detailed rotor models were developed to improve accuracy and to account for various design complexities such as gimbal mounts, swashplates, or bearingless root retention beams, among many others. The relevant equations of motion were derived for the specific configurations at hand. In fact, the various codes developed in-house by rotorcraft manufacturers are geared towards the modeling of the specific configuration they produce. This approach severely limits the generality and flexibility of the resulting codes.

In recent years, a number of new rotorcraft configurations have been proposed: bearingless rotors with redundant load paths, tilt rotors, co-axial rotors, or variable diameter tilt rotors, to name just a few. Developing a new simulation tool for each novel configuration is a daunting task, and software validation is an even more difficult issue. Furthermore, the requirement for ever more accurate predictions calls for increasingly detailed and comprehensive models. For instance, modeling the interaction of the rotor with a flexible fuselage or with the control chain must be considered to capture specific phenomena or instabilities.

The finite element based flexible multibody dynamics formulation outlined above appears to be readily applicable to the rotorcraft dynamics analysis, because a rotorcraft system can be viewed as a complex flexible mechanism. It is now becoming the industry norm for this complex, nonlinear problem.

Figure 15.2 depicts the conceptual representation of a rotorcraft system as a flexible multibody system. The various mechanical components of the system are associated with elements found in the library of typical multibody analysis tools. The figure shows a classical configuration for the control chain, consisting of a swashplate with rotating and non-rotating components. The lower swashplate motion is controlled by actuators that provide the vertical and angular control inputs. The upper swashplate is connected to the rotor shaft through a scissors-like mechanism and controls the blade pitching motions through pitch-links.

This control linkage configuration can be modeled using the following elements: rigid bodies, used to model the non-rotating and rotating swashplate components and

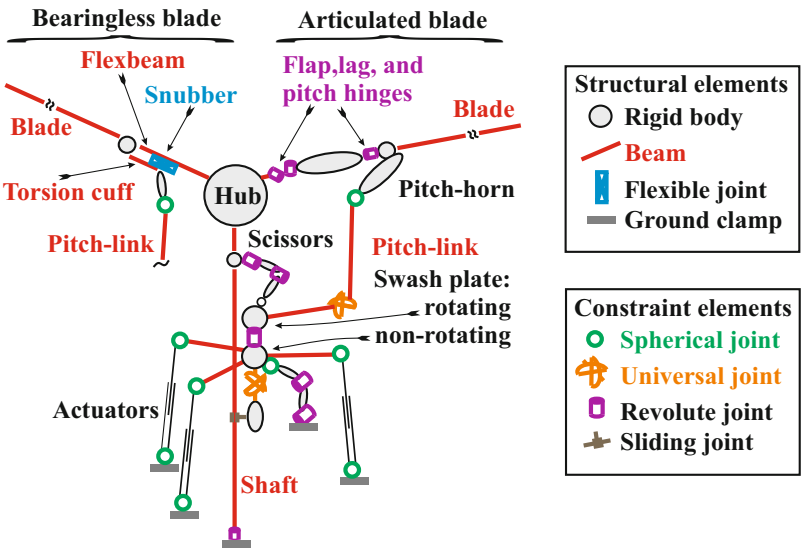

Fig. 15.2. Detailed multibody representation of a rotor system.

scissors links, and beams for modeling the flexible shaft and pitch-link. These bodies are connected through mechanical joints. For instance, a revolute joint, described in section 10.6.1, connects the rotating and non-rotating swashplates, allowing the former to rotate at the shaft angular velocity while the latter is non-rotating. Revolute joints also connect the scissors links to each other and to the upper swashplate, thereby synchronizing the angular speeds of the shaft and upper swashplate.

Other types of joints are required for the model. For instance, the non-rotating swashplate is allowed to tilt with respect to an element that slides along the shaft, but does not rotate about the shaft direction. The universal joint, described in section 10.7.1, serves this purpose. Similarly, the pitch-link is connected to the pitch-horn by means of a spherical joint, see section 10.6.6, that allows the connected components to be at an arbitrary orientation with respect to each other. The other end of the pitch-link is attached to the swashplate by means of a universal joint.

Figure 15.2 also shows two different rotor configurations: a classical, fully articulated design on the right portion of the figure and a bearingless design on the left. The articulated blade is connected to the hub through three consecutive revolute joints, that allow out-of-plane, in-plane, and torsional motions of the blade. For rotorcraft, these joints are called the flap, lag, and pitch hinges, respectively. In some designs, these joints are collocated, while other designs call for offset distances between these joints. In the latter case, rigid or flexible bodies of finite dimensions would be used to connect the three joints.

For bearingless designs, the blade connects to the hub through a flexible component, called the flexbeam. The control input coming from the pitch-link is transmitted to the blade via the torsion cuff, represented by a flexible beam. To ensure a purely

rotational motion of the torsion cuff, it is also connected to the flexbeam through a snubber, which is typically modeled as a flexible joint, see section 16.1. The bearingless design is a multiple load path configuration: the flexbeam and torsion cuff are assembled in parallel and connected by a snubber.

Because they eliminates the flap, lag, and pitch hinges characteristic of fully articulated designs, bearingless designs are mechanically simpler and more robust. On the other hand, the blade's control motions are accommodated through flexible elements, which could be subjected to higher stresses than those observed in fully articulated design.

When using the finite element based flexible multibody dynamics formulation outlined above, the two designs, fully articulated and bearingless, can be modeled by assembling different sets of elements from the multibody library of elements. There is no need to derive and validate two different sets of equations for the two configurations.

The blade itself is modeled by an appropriate beam element that should account for shearing deformations and for all elastic couplings that arise from the use of composite materials [283]. Furthermore, the center of mass, center of tension, and shear center of the blade are at distinct geometric locations of the blade's cross-section, further complicating the modeling task.

Of course, the level of detail presented in fig. 15.2 is not always needed: some or all of the control chain components could be omitted, and the blade could be represented by a rigid body rather than beam elements, if a crude model is desired.

15.2 The elastodynamics problem

Figure 15.3 depicts an elastic body of arbitrary shape subjected to time-dependent surface tractions and body forces. Geometric boundary conditions consist of time-dependent prescribed displacements at a point or over a portion of the body's outer surface. The volume of the body is denoted $\mathcal{V}$ and its outer surface $\mathcal{S}$. Unit vector $\bar{n}$ is the normal to its outer surface. The dynamic response of the system is studied between initial and a final times, denoted t_i and t_f, respectively. The displacement field at a point of the body is denoted $\underline{u}(x_1, x_2, x_3, t)$, where t denotes time and x_1, x_2, and x_3 the Cartesian coordinates of a point of the body resolved in inertial frame $\mathcal{F}^I = [\mathbf{O}, \mathcal{I} = (\bar{\imath}_1, \bar{\imath}_2, \bar{\imath}_3)]$.

Over the outer surface of the body, displacements and surface tractions are denoted $\hat{\underline{u}}(t)$ and $\hat{\underline{t}}(t)$, respectively. Over portion $\mathcal{S}_1$ of the body's outer surface, the surface tractions are given, prescribed quantities; this includes the portion of the outer surface that is traction free, because vanishing surface tractions, $\hat{\underline{t}}(t) = 0$, are prescribed over that portion of the outer surface. Over portion $\mathcal{S}_2$ of the body's outer surface, the displacements are given, prescribed quantities.

Surfaces $\mathcal{S}_1$ and $\mathcal{S}_2$ share no common point because *displacements and tractions cannot be prescribed simultaneously* at the same point, and hence, $\mathcal{S} = \mathcal{S}_1 + \mathcal{S}_2$. Over $\mathcal{S}_1$, $\hat{\underline{t}}(t)$ represents the prescribed surface tractions, and $\underline{\hat{u}}(t)$ the resulting displacements. Over $\mathcal{S}_2$, $\hat{\underline{u}}(t)$ represents the prescribed displacements, and $\underline{\hat{t}}(t)$ the resulting

traction, also called *reaction forces*. Reaction forces are those forces arising from the enforcement of the prescribed displacements.

At the initial and final times, the momenta and displacements are denoted $\hat{\underline{p}}$ and $\hat{\underline{u}}$, respectively. At these times, displacements could be given, prescribed quantities, and simultaneously, momenta could also be given, prescribed quantities. Note that at the initial and final times, *both displacements and momenta can be prescribed simultaneously*. For instance, in an initial value problem, both initial displacements and momenta are prescribed at the initial time, and the values of both quantities at the final time will result from the analysis.

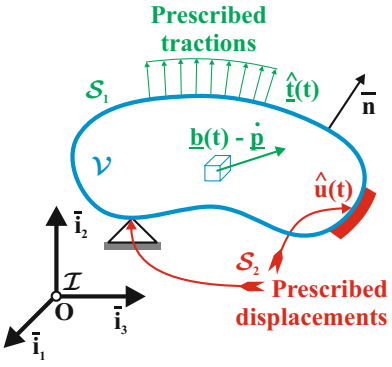

Fig. 15.3. General elastodynamics problem.

Time-dependent body forces, $\underline{b}(t)$, might also be applied over the entire volume of the body. Gravity forces are a typical example of body forces, but such forces can also arise from electric or magnetic fields. In dynamic problems, inertial forces can be considered to be externally applied body forces, in accordance with d'Alembert's principle. The momentum vector for a differential element of the body is $\underline{p} = \rho \underline{v}$, where ρ is the material mass density and $\underline{v}$ the element's inertial velocity vector. The inertial forces are then $-\dot{\underline{p}}$.

The basic equations of elastodynamics form a set of first-order partial differential equations in space and time that can be solved to find the displacement, velocity, strain, stress, and momentum fields at all points of the body and all instants in time. These equations will be reviewed in section 15.2.1 where several important definitions are also introduced. In the subsequent sections, a number of variational and energy principles are presented that provide an alternative formalism for the solution of elasticity problems. This formalism is the basis for powerful numerical techniques, such as the *finite element method*, that are routinely used to obtain approximate solutions to complex elastodynamics problems.

15.2.1 Review of the equations of linear elastodynamics

As discussed in section 8.1, d'Alembert's principle reduces dynamics problems to statics problems, provided that inertial forces are treated as externally applied forces. This implies that elastodynamics problems reduce to elasticity problems, provided that inertial forces are treated as externally applied forces. The equations presented in this section are, in fact, the general equations of elasticity [284, 285], in which the inertial forces taken into account as externally applied body forces. The equations of elastodynamics can be broken into three groups: *(1)* the equations of dynamic equilibrium, *(2)* the strain-displacement and velocity-displacement equations, and *(3)* the constitutive laws.

The equations of dynamic equilibrium

The *equations of dynamic equilibrium* are the most fundamental equations of elasticity. They are derived from Newton's first law, see section 3.1.2, which states the conditions for static equilibrium of a differential element of the body. D'Alembert's principle 12 then states the conditions for dynamic equilibrium of the differential element of the body,

$$\frac{\partial \sigma_1}{\partial x_1} + \frac{\partial \tau_{21}}{\partial x_2} + \frac{\partial \tau_{31}}{\partial x_3} + b_1 - \dot{p}_1 = 0, \tag{15.1a}$$

$$\frac{\partial \tau_{12}}{\partial x_1} + \frac{\partial \sigma_2}{\partial x_2} + \frac{\partial \tau_{32}}{\partial x_3} + b_2 - \dot{p}_2 = 0, \tag{15.1b}$$

$$\frac{\partial \tau_{13}}{\partial x_1} + \frac{\partial \tau_{23}}{\partial x_2} + \frac{\partial \sigma_3}{\partial x_3} + b_3 - \dot{p}_3 = 0, \tag{15.1c}$$

where σ_1, σ_2, and σ_3 are the *direct stress* components and τ_{23}, τ_{13}, and τ_{12} the *shear stress* components. These are the components of the stress tensor [284, 285] resolved in basis $\mathcal{I}$. The components of the body force and momentum vectors were resolved in the inertial basis as $\underline{b}^T = \{b_1, b_2, b_3\}$ and $\underline{p}^T = \{p_1, p_2, p_3\}$, respectively. Equations (15.1) are first-order, partial differential equations in space and time must be satisfied at all points of the body and all instants in time.

The *surface equilibrium equations* state that at all points on $\mathcal{S}$ and all instants in time,

$$t_1 = n_1\sigma_1 + n_2\tau_{21} + n_3\tau_{31} = \hat{t}_1, \tag{15.2a}$$

$$t_2 = n_1\tau_{12} + n_2\sigma_2 + n_3\tau_{32} = \hat{t}_2, \tag{15.2b}$$

$$t_3 = n_1\tau_{13} + n_2\tau_{23} + n_3\sigma_3 = \hat{t}_3, \tag{15.2c}$$

where the components of the unit vector normal to the outer surface of the body, the surface traction vector, and the prescribed surface traction vector, all resolved in basis $\mathcal{I}$, are denoted $\underline{n}^T = \{n_1, n_2, n_3\}$, $\underline{t}^T = \{t_1, t_2, t_3\}$, and $\hat{\underline{t}}^T = \{\hat{t}_1, \hat{t}_2, \hat{t}_3\}$, respectively. Over $\mathcal{S}_1$, these conditions are also called the *force*, or *natural boundary conditions*. The stress array

$$\underline{\sigma}^T(t) = \{\sigma_1, \sigma_2, \sigma_3, \tau_{23}, \tau_{13}, \tau_{12}\}, \tag{15.3}$$

will be used whenever that notation is convenient to represent the stress field.

Finally, additional conditions are imposed on the momentum vectors at the initial and final times

$$\underline{p}(t_i) = \hat{\underline{p}}_i, \quad \underline{p}(t_f) = \hat{\underline{p}}_f. \tag{15.4}$$

These conditions are called the *boundary conditions in time.*

Definition 15.1 (Admissible stress and momentum fields). *Stress fields, $\underline{\sigma}(x_1, x_2, x_3, t)$, and momentum fields, $\underline{p}(x_1, x_2, x_3, t)$, are said to be admissible if, at all times, they satisfies the dynamic equilibrium equations, eqs.* (15.1)*, at all points in $\mathcal{V}$, the surface equilibrium equations, eqs.* (15.2)*, at all points on $\mathcal{S}$, and the time boundary conditions, eqs.* (15.4)*, at times t_i and t_f.*

The strain-displacement and velocity-displacement relationships

The *strain-displacement equations* merely define the strain components that are used for the characterization of the deformation of the body at a point. The strain-displacement relationships are derived from purely geometric considerations. Similarly, the *velocity-displacement equations* simply define the velocity components at a point of the body.

When the displacements are small, deformations at a point of the body are conveniently measured by the engineering strain components [284, 285], defined as,

$$\varepsilon_1 = \frac{\partial u_1}{\partial x_1}, \qquad \varepsilon_2 = \frac{\partial u_2}{\partial x_2}, \qquad \varepsilon_3 = \frac{\partial u_3}{\partial x_3}, \tag{15.5a}$$

$$\gamma_{23} = \frac{\partial u_2}{\partial x_3} + \frac{\partial u_3}{\partial x_2}, \quad \gamma_{13} = \frac{\partial u_1}{\partial x_3} + \frac{\partial u_3}{\partial x_1}, \quad \gamma_{12} = \frac{\partial u_1}{\partial x_2} + \frac{\partial u_2}{\partial x_1}, \tag{15.5b}$$

where ε_1, ε_2, and ε_3 are the *relative elongations* or *direct strain* components of a material line and γ_{23}, γ_{13}, and γ_{12} the *angular distortions* or *shear strain* components of two material lines.

To compute strain components, the displacement field must be continuous and differentiable. Furthermore, over $\mathcal{S}$ and at the initial and final times, the following *displacement boundary conditions* must be met

$$\underline{u}(t) = \hat{\underline{u}}(t). \tag{15.6}$$

Over $\mathcal{S}_2$, these conditions are called the *geometric boundary conditions*. The strain array

$$\underline{\varepsilon}^T(t) = \left\{\varepsilon_1,\ \varepsilon_2,\ \varepsilon_3,\ \gamma_{23},\ \gamma_{13},\ \gamma_{12}\right\}, \tag{15.7}$$

will be used whenever that notation is convenient to represent the strain field.

The components of the velocity vector $\underline{v}(t)$ are the time derivatives of the displacement vector,

$$\underline{v}(t) = \dot{\underline{u}}. \tag{15.8}$$

Definition 15.2 (Kinematically admissible displacement field). *A displacement field, $\underline{u}(x_1, x_2, x_3, t)$, is said to be kinematically admissible if, at all time, it is continuous and differentiable at all points in $\mathcal{V}$ and satisfies the displacement boundary conditions, eqs.* (15.6)*, at all points on $\mathcal{S}$ and the initial and final times.*

Definition 15.3 (Compatible strain field). *A strain field, $\underline{\varepsilon}(x_1, x_2, x_3, t)$, is said to be compatible if, at all times, it is derived from a kinematically admissible displacement field through the strain-displacement relationships, eqs.* (15.5)*.*

Definition 15.4 (Compatible velocity field). *A velocity field, $\underline{v}(x_1, x_2, x_3, t)$, is said to be compatible if, at all times, it is derived from a kinematically admissible displacement field through the velocity-displacement relationships, eqs.* (15.8)*.*

The constitutive laws

The *constitutive laws* relate the stress and strain fields. They consist of a mathematical idealization of the experimentally observed behavior of materials. Hooke's law is commonly used to model the behavior of homogeneous, isotropic, linearly elastic materials operating in the small strain regime. Many materials may present one or more of the following features: anisotropy, plasticity, visco-elasticity, or creep, to name just a few commonly observed behaviors of engineering materials. A second set of constitutive laws relates the momentum vector to the velocity vector.

The stress and strain fields must satisfy the constitutive laws at all points in $\mathcal{V}$. For small strains, Hooke's law [284, 285] represents the behavior of homogeneous, isotropic, linearly elastic materials in a approximate manner by the following linear relationship

$$\underline{\sigma} = \underline{\underline{C}}\,\underline{\varepsilon}, \quad \underline{\varepsilon} = \underline{\underline{S}}\,\underline{\sigma}, \tag{15.9}$$

where $\underline{\underline{C}}$ is a symmetric, positive-definite *material stiffness matrix*, and $\underline{\underline{S}} = \underline{\underline{C}}^{-1}$ a symmetric, positive-definite *material compliance matrix*.

A constitutive law is also required for the momentum field. This law is, in fact, the definition of the momentum vector

$$\underline{p} = \rho\,\underline{v}, \tag{15.10}$$

where ρ is the material mass density.

Summary

Complete solutions of elastodynamics problems involves the following fields.

1. Admissible stress and momentum fields, see definition 15.1.
2. Kinematically admissible displacement fields, see definition 15.2, and associated compatible strain and velocity fields, see definition 15.3 and 15.4, respectively.
3. Stress and momentum fields that satisfy the constitutive laws, eqs. (15.9) and (15.10), respectively, at all points in $\mathcal{V}$.

All these equations must be satisfied at all instants in time.

15.2.2 The principle of virtual work

Consider an elastic body that is in dynamic equilibrium under applied body forces and surface tractions. This implies that the stress and momentum fields are admissible, see definition 15.1. The following statement is now constructed

$$\begin{aligned}\int_{t_i}^{t_f}\int_{\mathcal{V}}\Big[&(\frac{\partial\sigma_1}{\partial x_1}+\frac{\partial\tau_{21}}{\partial x_2}+\frac{\partial\tau_{31}}{\partial x_3}+b_1-\dot{p}_1)\,\delta u_1\\&+(\frac{\partial\tau_{12}}{\partial x_1}+\frac{\partial\sigma_2}{\partial x_2}+\frac{\partial\tau_{32}}{\partial x_3}+b_2-\dot{p}_2)\,\delta u_2\\&+(\frac{\partial\tau_{13}}{\partial x_1}+\frac{\partial\tau_{23}}{\partial x_2}+\frac{\partial\sigma_3}{\partial x_3}+b_3-\dot{p}_3)\,\delta u_3\Big]\,\mathrm{d}\mathcal{V}\mathrm{d}t\\-\int_{t_i}^{t_f}\int_{\mathcal{S}}(\underline{t}-\hat{\underline{t}})^T\delta\underline{u}\,\mathrm{d}\mathcal{S}\mathrm{d}t&+\Big[\int_{\mathcal{V}}(\underline{p}-\hat{\underline{p}})^T\delta\underline{u}\,\mathrm{d}\mathcal{V}\Big]_{t_i}^{t_f}=0.\end{aligned}\tag{15.11}$$

This statement was constructed in the following manner. Each of the three dynamic equilibrium equations, eqs. (15.1), was multiplied by an arbitrary, virtual change in displacement, then integrated over the range of validity of the equation. Similarly, each of the three surface equilibrium equations, eqs. (15.2), was multiplied by an arbitrary, virtual change in displacement, then integrated over the range of validity of the equation. Finally, each of the three boundary conditions in time, eqs. (15.4), was multiplied by an arbitrary, virtual change in displacement, then integrated over the range of validity of the equation.

Because the stress and momentum fields are admissible, each term in parenthesis is zero, and multiplication by an arbitrary quantity results in a zero product. Each of the three integrals then vanishes, as does their sum.

Next, integration by parts is performed. Using Green's theorem [2], the first term of the volume integral becomes

$$\int_{\mathcal{V}}\frac{\partial\sigma_1}{\partial x_1}\,\delta u_1\,\mathrm{d}\mathcal{V}=-\int_{\mathcal{V}}\sigma_1\frac{\partial\delta u_1}{\partial x_1}\,\mathrm{d}\mathcal{V}+\int_{\mathcal{S}}n_1\sigma_1\,\delta u_1\,\mathrm{d}\mathcal{S},$$

where n_1 is the component of the outward unit normal along $\bar{\imath}_1$, see fig. 15.3. A similar operation is performed on each stress derivative terms appearing in eq. (15.11). For the momentum terms, integration by parts yields

$$-\int_{t_i}^{t_f}\dot{\underline{p}}^T\delta\underline{u}\,\mathrm{d}t=\int_{t_i}^{t_f}\underline{p}^T\delta\dot{\underline{u}}\,\mathrm{d}t-\left[\underline{p}^T\delta\underline{u}\right]_{t_i}^{t_f}=\int_{t_i}^{t_f}\underline{p}^T\delta\underline{v}\,\mathrm{d}t-\left[\underline{p}^T\delta\underline{u}\right]_{t_i}^{t_f}.$$

Introducing the results of these integrations by parts into eq. (15.11) then yields

$$\begin{aligned}-\int_{t_i}^{t_f}\Big\{\int_{\mathcal{V}}\left[\underline{\sigma}^T\delta\underline{\varepsilon}+\underline{p}^T\delta\underline{v}\right]\,\mathrm{d}\mathcal{V}+\int_{\mathcal{V}}\underline{b}^T\delta\underline{u}\,\mathrm{d}\mathcal{V}+\int_{\mathcal{S}}\hat{\underline{t}}^T\delta\underline{u}\,\mathrm{d}\mathcal{S}\Big\}\,\mathrm{d}t\\-\Big[\int_{\mathcal{V}}\hat{\underline{p}}^T\delta\underline{u}\,\mathrm{d}\mathcal{V}\Big]_{t_i}^{t_f}=0,\end{aligned}\tag{15.12}$$

where the *virtual, compatible strain field* was defined as

$$\delta\varepsilon_1=\frac{\partial\delta u_1}{\partial x_1},\qquad\delta\varepsilon_2=\frac{\partial\delta u_2}{\partial x_2},\qquad\delta\varepsilon_3=\frac{\partial\delta u_3}{\partial x_3},\tag{15.13a}$$

$$\delta\gamma_{23}=\frac{\partial\delta u_2}{\partial x_3}+\frac{\partial\delta u_3}{\partial x_2},\ \delta\gamma_{13}=\frac{\partial\delta u_1}{\partial x_3}+\frac{\partial\delta u_3}{\partial x_1},\ \delta\gamma_{12}=\frac{\partial\delta u_1}{\partial x_2}+\frac{\partial\delta u_2}{\partial x_1},\tag{15.13b}$$

and the *virtual, compatible velocity field* as

$$\delta \underline{v} = \delta \dot{\underline{u}}. \tag{15.14}$$

Equation (15.12) can be restated as

$$\begin{aligned} &-\int_{t_i}^{t_f} \int_{\mathcal{V}} \left[\underline{\sigma}^T \delta \underline{\varepsilon} - \underline{p}^T \delta \underline{v} \right] \, \mathrm{d}\mathcal{V}\mathrm{d}t \\ &+\int_{t_i}^{t_f} \left\{ \int_{\mathcal{V}} \underline{b}^T \delta \underline{u} \, \mathrm{d}\mathcal{V} + \int_{\mathcal{S}} \hat{\underline{t}}^T \delta \underline{u} \, \mathrm{d}\mathcal{S} \right\} \mathrm{d}t - \left[\int_{\mathcal{V}} \underline{\hat{p}}^T \delta \underline{u} \, \mathrm{d}\mathcal{V} \right]_{t_i}^{t_f} = 0. \end{aligned} \tag{15.15}$$

The first term represents the virtual work done by the internal stresses and momenta and the remaining correspond to the virtual work done by the externally applied loads and momenta.

It has been shown thus far that if the stress and momenta fields are admissible, eq. (15.15) must hold. It can also be shown that if this equation holds, the stress and momenta fields must be admissible. Indeed, eq. (15.15) implies eq. (15.12), which in turns implies eq. (15.11) by reversing the integration by parts process. Finally, the volume and surface equilibrium equations are recovered because eq. (15.11) must hold for all arbitrary, kinematically admissible virtual displacements fields. Statement (15.15) can thus be interpreted as follows.

Principle 19 (Principle of virtual work) *A body is in dynamic equilibrium if the sum of the internal and external virtual work vanishes for all arbitrary kinematically admissible virtual displacement fields and corresponding compatible strain and velocity fields.*

This principle is illustrated in fig. 15.4. The surface tractions act at the spatial boundaries of the problem and play a role similar to that of the momenta at the temporal boundaries of the problem.

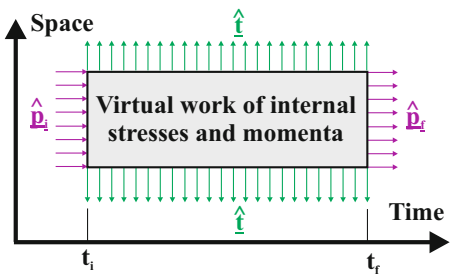

Fig. 15.4. Illustration of the principle of virtual work.

In summary, the equations of dynamic equilibrium, eqs. (15.1), (15.2), and (15.4), and the principle of virtual work are two equivalent statements. Furthermore, because the equations of dynamic equilibrium are a statement of Newton's second law, the principle of virtual work and Newton's second law are two equivalent statements.

Because the principle of virtual work is solely a statement of equilibrium, it is always true. However, for the solution of specific elastodynamics problems, it must be complemented with stress-strain and momentum-velocity relationships, and constitutive laws. More details about the principle of virtual work and its application to structures can be found in numerous textbooks such as [284, 286, 287, 285].

15.2.3 Hamilton's principle

If the internal forces in the solid are assumed to be conservative, they can be derived from a potential, as discussed in section 3.2. In this case, the internal forces are the components of stress, and the potential is the *strain energy density function*. If the stresses in the solid can be derived from a strain energy density function, $a(\underline{\epsilon})$,

$$\underline{\sigma} = \frac{\partial a(\underline{\varepsilon})}{\partial \underline{\varepsilon}}, \tag{15.16}$$

the material is said to be an *elastic material*. Assuming the material to be elastic or assuming the existence of a strain energy density function are two equivalent assumptions. Linearly elastic materials are elastic materials for which the stress-strain relationship is linear.

If the material is elastic, the work done by the internal stresses when the system is brought from one state of deformation to another depends only on the two states of deformations, but not on the specific path that the system followed from one deformation state to the other. This restricts the types of material constitutive laws that can be expressed in terms of a strain energy density function. For instance, if a material is deformed in the plastic range, the work of deformation will depend on the specific deformation history; hence, there exists no strain energy density function that describes material behavior when plastic deformations are involved.

For instance, the strain energy density function of a linearly elastic material is

$$a(\underline{\varepsilon}) = \frac{1}{2}\underline{\varepsilon}^T \underline{\underline{C}}\, \underline{\varepsilon}. \tag{15.17}$$

Introducing this function into eq. (15.16), yields $\underline{\sigma} = \underline{\underline{C}}\, \underline{\varepsilon}$, the constitutive law for a linearly elastic material.

Consider a general elastic body that is in equilibrium under applied body forces and surface tractions, and therefore, the principle of virtual work, eq. (15.15), must apply. It is now assumed that the constitutive law for the material can be expressed in terms of a strain energy density function, eq. (15.16). The virtual work done by the internal stresses appears in the first term of eq. (15.15), and it is readily evaluated as

$$\int_{\mathcal{V}} \delta\underline{\varepsilon}^T \underline{\sigma}\, \mathrm{d}\mathcal{V} = \int_{\mathcal{V}} \delta\underline{\varepsilon}^T \frac{\partial a(\underline{\varepsilon})}{\partial \underline{\varepsilon}}\, \mathrm{d}\mathcal{V} = \int_{\mathcal{V}} \delta a(\underline{u})\, \mathrm{d}\mathcal{V} = \delta \int_{\mathcal{V}} a(\underline{u})\, \mathrm{d}\mathcal{V} = \delta A(\underline{u}),$$

where the chain rule for derivatives is used to obtain the second equality.

The strain energy density and the *total strain energy* of the body, $A = \int_{\mathcal{V}} a\, \mathrm{d}\mathcal{V}$, must be expressed in terms of the displacement field using the strain-displacement relationships because the principle of virtual work requires a compatible strain field.

In a similar manner, the use of the dynamic constitutive law, eq. (15.10), leads to

$$\int_{\mathcal{V}} \underline{p}^T \delta\underline{v}\, \mathrm{d}\mathcal{V} = \int_{\mathcal{V}} \rho\underline{v}^T \delta\underline{v}\, \mathrm{d}\mathcal{V} = \int_{\mathcal{V}} \delta k(\underline{v})\, \mathrm{d}\mathcal{V} = \delta K(\underline{v}),$$

where $k(\underline{v}) = 1/2\ \rho\underline{v}^T\underline{v}$ is the *kinetic energy density function*, and $K(\underline{v})$ the *total kinetic energy* of the body.

The principle of virtual work, eq. (15.15), now becomes

$$\begin{aligned} &-\delta \int_{t_i}^{t_f} (A - K)\, \mathrm{d}t \\ &+ \int_{t_i}^{t_f} \left\{ \int_{\mathcal{V}} \underline{b}^T \delta \underline{u}\, \mathrm{d}\mathcal{V} + \int_{\mathcal{S}} \hat{\underline{t}}^T \delta \underline{u}\, \mathrm{d}\mathcal{S} \right\} \mathrm{d}t - \left[\int_{\mathcal{V}} \underline{\hat{p}}^T \delta \underline{u}\, \mathrm{d}\mathcal{V} \right]_{t_i}^{t_f} = 0. \end{aligned} \tag{15.18}$$

The first term on the second line of this statement represents the *virtual work done by the externally applied loads*,

$$\delta W_{\mathrm{ext}} = \int_{\mathcal{V}} \underline{b}^T \delta \underline{u}\, \mathrm{d}\mathcal{V} + \int_{\mathcal{S}} \hat{\underline{t}}^T \delta \underline{u}\, \mathrm{d}\mathcal{S}. \tag{15.19}$$

With this definition, the principle of virtual work, eq. (15.18), becomes

$$-\delta \int_{t_i}^{t_f} (A - K)\, \mathrm{d}t + \int_{t_i}^{t_f} \delta W_{\mathrm{ext}}\, \mathrm{d}t - \left[\int_{\mathcal{V}} \underline{\hat{p}}^T \delta \underline{u}\, \mathrm{d}\mathcal{V} \right]_{t_i}^{t_f} = 0. \tag{15.20}$$

Next, the body forces and surface tractions are assumed to be conservative, *i.e.*, they can be derived from a potential,

$$\underline{b} = -\frac{\partial \phi}{\partial \underline{u}}; \quad \hat{\underline{t}} = -\frac{\partial \psi}{\partial \underline{u}},$$

where ϕ is the *potential of the body forces*, and ψ the *potential of the surface tractions*. For instance, the potential of fixed surface tractions is simply $\psi = -\hat{\underline{t}}^T \underline{u}$, or the potential of the body forces associated with a gravity field, $\underline{g}$, is $\phi = -\rho\, \underline{g}^T \underline{u}$.

The two terms of the virtual work done by the external forces, eq. (15.19), now become

$$\begin{aligned} \int_{\mathcal{V}} \underline{b}^T \delta \underline{u}\, \mathrm{d}\mathcal{V} &= -\int_{\mathcal{V}} \frac{\partial \phi}{\partial \underline{u}}^T \delta \underline{u}\, \mathrm{d}\mathcal{V} = -\delta \int_{\mathcal{V}} \phi(\underline{u})\, \mathrm{d}\mathcal{V}, \\ \int_{\mathcal{S}} \hat{\underline{t}}^T \delta \underline{u}\, \mathrm{d}\mathcal{S} &= -\int_{\mathcal{S}} \frac{\partial \psi}{\partial \underline{u}}^T \delta \underline{u}\, \mathrm{d}\mathcal{S} = -\delta \int_{\mathcal{S}} \psi(\underline{u})\, \mathrm{d}\mathcal{S}. \end{aligned}$$

Combining these two loading terms then yields

$$\delta W_{\mathrm{ext}} = -\delta \int_{\mathcal{V}} \phi(\underline{u})\, \mathrm{d}\mathcal{V} - \delta \int_{\mathcal{S}} \psi(\underline{u})\, \mathrm{d}\mathcal{S} = -\delta \Phi(\underline{u}),$$

where $\Phi(\underline{u})$ is the *total potential the externally applied loads*. Introducing this result into eq. (15.20) leads to

$$\delta \int_{t_i}^{t_f} (A - K + \Phi)\, \mathrm{d}t + \left[\int_{\mathcal{V}} \underline{\hat{p}}^T \delta \underline{u}\, \mathrm{d}\mathcal{V} \right]_{t_i}^{t_f} = 0. \tag{15.21}$$

The *Lagrangian* of the system is now defined as

$$L = K(\underline{v}) - A(\underline{u}) - \Phi(\underline{u}), \tag{15.22}$$

and it follows that

$$\int_{t_i}^{t_f} \delta L \, \mathrm{d}t = \left[\int_{\mathcal{V}} \underline{\hat{p}}^T \delta \underline{u} \, \mathrm{d}\mathcal{V} \right]_{t_i}^{t_f} \tag{15.23}$$

Hamilton's principle can be stated as

Principle 20 (Hamilton's principle) *An elastic system is in dynamic equilibrium if and only if equation* (15.23) *holds for all arbitrary virtual displacements.*

Clearly, this statement generalizes the version of Hamilton's principle derived in section 8.2 for systems of particles. If the momenta vanish at the initial and final times, it simply becomes $\delta L = 0$.

Many other variational principles exist in elasticity. Particularly noteworthy are the principle of complementary virtual work and the principle of minimum complementary energy [286, 287, 285]. Two or three field principles can also be developed, such as Hellinger-Reissner's and Hu-Washizu's principles, respectively. All these principle can be extended to elastodynamics problem by invoking d'Alembert's principle, inertial forces are included as externally applied forces.

15.3 Finite displacements kinematics for flexible bodies

While flexible multibody systems are characterized by large relative motions at the joints, it is often the case that individual flexible bodies undergo small deformations. Conceptually, the displacement field at a point of the flexible body can be decomposed into rigid body and elastic displacement field [167], where the latter field is responsible for the straining of the body whereas the former, by definition, generates no deformation.

It is not uncommon for structures such as slender beams or thin plates and shells, to undergo large rigid body displacements and rotations while the strains remain small at all points of the structure. This behavior is often the consequence of careful planning: to avoid premature failure, the structure is designed to operate in the small strain regime.

When a structure operates in the small strain regime, the three groups of equations of elastodynamics described in section 15.2.1 still apply, but must be updated to account for the large displacements. Of course, Newton's law still applies, but in this case, the equilibrium conditions must be enforced on the deformed configuration of the structure. The strain-displacement relationships now become nonlinear equations, rather than the linear relationships that characterize small displacement problems, eqs. (15.5). Finally, the constitutive laws remain unchanged, although the stress and strain components are now those resolved in the *convected* or *material basis*.

This section presents a brief discussion of the state of deformation in the neighborhood of a material point in a flexible body. Two configuration of this body will be defined: a *reference configuration*, and a *deformed configuration*. The following notational convention will be used: lower-case symbols refer to quantities defined

in the reference configuration, and upper-case symbols refer to the corresponding quantities in the deformed configuration.

Material coordinates

Figure 15.5 depicts a body in its reference and deformed configurations and an inertial frame, $\mathcal{F}^I = [\mathbf{O}, \mathcal{I} = (\bar{\imath}_1, \bar{\imath}_2, \bar{\imath}_3)]$. This section focuses on the relationships between the deformed and reference configuration of the solid without any consideration for the loads that create the deformation.

Let point **P** be a material point of the body, and the position vectors of this material point are denoted $\underline{x}$ and $\underline{X}$, in the reference and deformed configuration, respectively. Each material particle of the body will be identified by a label consisting of a triplet of real numbers. This label will remain attached to the material particle throughout the deformation process. This label is called the *material coordinates* of material point **P**, and is denoted $(\alpha_1, \alpha_2, \alpha_3)$.

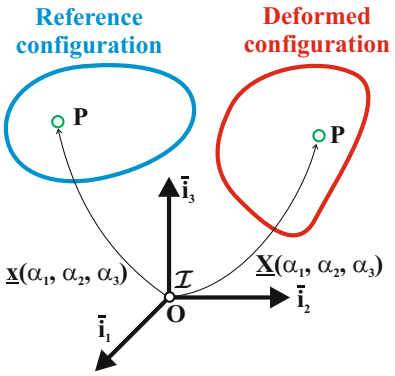

Fig. 15.5. The reference and deformed configurations of a body.

The position vectors of point **P** in the reference and deformed configurations are

$$\underline{x} = \underline{x}(\alpha_1, \alpha_2, \alpha_3), \tag{15.24a}$$

$$\underline{X} = \underline{X}(\alpha_1, \alpha_2, \alpha_3), \tag{15.24b}$$

respectively. Because the material coordinates are an identifying label for a material particle, they can be chosen arbitrarily. A convenient choice for the material coordinates consists of the components of the position vector resolved in basis $\mathcal{I}$

$$\underline{x}(\alpha_1, \alpha_2, \alpha_3) = \alpha_1\, \bar{\imath}_1 + \alpha_2\, \bar{\imath}_2 + \alpha_3\, \bar{\imath}_3. \tag{15.25}$$

This particular choice of the material coordinates is called the *Lagrangian representation.*

A *material line* is an ensemble of material particles forming a straight line in the reference configuration of the body. For instance, fig. 15.6 shows segments **PR**, **PS**, and **PT** of the reference configuration, which are are material lines intersecting at point **P**. Due to the deformation of the body, all the material particles forming material line **PR** will move to segment **PR** in the deformed configuration. Because segment **PR** is of differential length, it can be assumed to remain straight in the deformed configuration.

Base vectors and metric tensor

The *base vectors* are vectors tangent to these material line

$$\bar{g}_i = \frac{\partial \underline{x}}{\partial \alpha_i} = \bar{\imath}_i. \tag{15.26}$$

In the reference configuration, the base vectors are mutually orthogonal unit vectors.

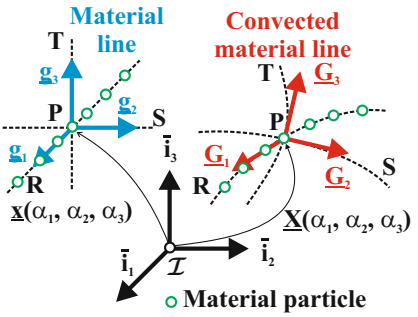

Fig. 15.6. The base vectors in the reference and deformed configurations.

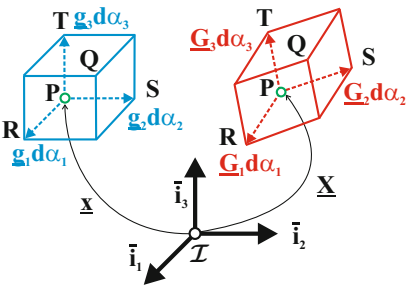

Fig. 15.7. Volume elements in the reference and deformed configurations.

As the deformation takes place, the material lines are convected with the body. The convected material lines now describe curves in space intersecting at the new location of the particle. The base vectors in the deformed configuration are defined in a manner similar to those of the reference configuration

$$\underline{G}_i = \frac{\partial \underline{X}}{\partial \alpha_i}. \tag{15.27}$$

These base vectors are not mutually orthogonal, nor are they unit vectors.

To visualize this deformation, fig. 15.7 shows the small rectangular parallelepiped **PQRST** of differential size $\mathrm{d}\alpha_1$ by $\mathrm{d}\alpha_2$ by $\mathrm{d}\alpha_3$ cut in the neighborhood of point **P**. The reference configuration is the configuration of the solid in its undeformed state, and rectangular parallelepiped **PQRST** is spanned by vectors $\bar{g}_1 \mathrm{d}\alpha_1$, $\bar{g}_2 \mathrm{d}\alpha_2$, and $\bar{g}_3 \mathrm{d}\alpha_3$. Under the action of applied loads, the body deforms and assumes a new configuration, called the deformed configuration. All the material particles that formed the rectangular parallelepiped **PQRST** in the reference configuration now form parallelepiped **PQRST**, which is spanned by vectors $\underline{G}_1 \mathrm{d}\alpha_1$, $\underline{G}_2 \mathrm{d}\alpha_2$, and $\underline{G}_3 \mathrm{d}\alpha_3$ in the deformed configuration. The state of strain at a point characterizes the deformation of the parallelepiped without any consideration for the loads that created the deformation.

Increments in position vector are denoted $\mathrm{d}\underline{x}$ and $\mathrm{d}\underline{X}$ in the reference and deformed configurations, respectively, and are expressed as

$$\mathrm{d}\underline{x} = \frac{\partial \underline{x}}{\partial \alpha_i}\, \mathrm{d}\alpha_i = \bar{g}_i\, \mathrm{d}\alpha_i,$$
$$\mathrm{d}\underline{X} = \frac{\partial \underline{X}}{\partial \alpha_i}\, \mathrm{d}\alpha_i = \underline{G}_i\, \mathrm{d}\alpha_i,$$

where summation is implied by the repeated indices.

The lengths of these increments, denoted $\mathrm{d}s$ and $\mathrm{d}S$ in the reference and deformed configurations, respectively, are readily found as

$$\mathrm{d}s^2 = \mathrm{d}\underline{x}^T \mathrm{d}\underline{x} = \bar{g}_i^T \bar{g}_j \, \mathrm{d}\alpha_i \mathrm{d}\alpha_j = g_{ij} \, \mathrm{d}\alpha_i \mathrm{d}\alpha_j, \tag{15.28a}$$

$$\mathrm{d}S^2 = \mathrm{d}\underline{X}^T \mathrm{d}\underline{X} = \underline{G}_i^T \underline{G}_j \, \mathrm{d}\alpha_i \mathrm{d}\alpha_j = G_{ij} \, \mathrm{d}\alpha_i \mathrm{d}\alpha_j. \tag{15.28b}$$

These relationships define the components of the *metric tensors* in the reference and deformed configurations, denoted g_{ij} and G_{ij}, respectively, as

$$g_{ij} = \bar{g}_i^T \bar{g}_j, \tag{15.29a}$$

$$G_{ij} = \underline{G}_i^T \underline{G}_j. \tag{15.29b}$$

The symmetry of both tensors is apparent from these definitions.

Displacement field

The difference between the positions of a material point in the deformed and reference configurations defines the *displacement vector* as

$$\underline{u}\,(\alpha_1, \alpha_2, \alpha_3) = \underline{X} - \underline{x}. \tag{15.30}$$

The displacement and position vectors in the deformed configuration are now resolved along the base vectors of the reference configuration as

$$\underline{u} = u_i \, \bar{g}_i, \tag{15.31a}$$

$$\underline{X} = X_i \, \bar{g}_i. \tag{15.31b}$$

With these definitions, eq. (15.30) now becomes

$$X_i = \alpha_i + u_i. \tag{15.32}$$

The base vector in the deformed configuration is related to the displacement field

$$\underline{G}_i = \frac{\partial \underline{X}}{\partial \alpha_i} = (\delta_{ij} + u_{j,i}) \, \bar{g}_j, \tag{15.33}$$

where δ_{ij} is Kronecker's symbol defined by eq. (1.14) and notation $(\cdot)_{,i}$ indicates a derivative with respect to material coordinate α_i.

Many different measures can be used to characterize the state of deformation at a point. Some measures are directly related to the physical concept of strain, *i.e.*, a relative change in length, but are not necessarily of a tensorial nature. Some other measures, clearly related to the physical concept of strain can be shown to be tensors.

15.3.1 The engineering strain components

The motion of segment **PR** from its reference to deformed configuration depicted in fig. 15.7 consists of two parts: a change in orientation and a change in length. Clearly, the change in length is a deformation or stretching of the material line. Similarly, segments **PR** and **PS** form a rectangle in the reference configuration, but form a parallelogram in the deformed configuration. The angular distortion of the rectangle into a parallelogram represents a deformation of the body. Stretching of a material line and angular distortion between two material lines will be selected as measures of the state of strain at a point.

The stretching or *relative elongations* of material lines **PR**, **PS**, and **PT** will be denoted as ε_1, ε_2, and ε_3, respectively. The *angular distortions* between segments **PS** and **PT**, **PR** and **PT**, and **PR** and **PS** will be denoted γ_{23}, γ_{13}, and γ_{12}, respectively.

The relative elongation, ε_1, of material line **PR**, see fig. 15.7, is defined as

$$\varepsilon_1 = \frac{\|\mathbf{PR}\|_{\mathrm{def}} - \|\mathbf{PR}\|_{\mathrm{ref}}}{\|\mathbf{PR}\|_{\mathrm{ref}}}, \tag{15.34}$$

where the subscripts $(\cdot)_{\mathrm{ref}}$ and $(\cdot)_{\mathrm{def}}$ are used to indicate the reference and deformed configurations, respectively. The relative elongation is a non-dimensional quantity. Similar definitions hold for ε_2 and ε_3, the relative elongation of material lines **PQ** and **PT**.

The angular distortion, γ_{23}, between two material lines **PT** and **PS** is defined as the change of the initially right angle, $\gamma_{23} = \pi/2 - \angle\mathbf{TPS}_{\mathrm{def}}$, where notation $\angle\mathbf{TPS}$ is used to indicate the angle between segments **PT** and **PS**. This can also written as

$$\gamma_{23} = \arcsin \frac{\underline{G}_2^T \underline{G}_3}{\|\underline{G}_2\| \, \|\underline{G}_3\|}. \tag{15.35}$$

Angular distortion are non-dimensional quantities. Similar definitions hold for the angular distortion γ_{13} and γ_{12} of the angles between material lines **PR** and **PT**, and **PS** and **PT**, respectively. The engineering strain components do not form a second-order tensor. They are often called *physical strain components.*

15.3.2 The deformation gradient tensor

A widely used strain measure is the *deformation gradient tensor* defined as

$$F_{ij} = \frac{\partial X_i}{\partial \alpha_j}. \tag{15.36}$$

In the following sections, the index notation will be used to represent second-order tensors. For instance, the deformation gradient tensor is denoted F_{ij} rather than the less explicit $\underline{\underline{F}} = \partial \underline{X} / \partial \underline{\alpha}$.

Resolving the base vector in the deformed configuration, eq. (15.27), along the reference frame yields

$$\underline{G}_i = \frac{\partial \underline{X}}{\partial \alpha_i} = F_{ji}\, \bar{g}_j. \tag{15.37}$$

A scalar product of this relationship by $\bar{g}_l$ yields an alternative definition of the deformation gradient tensor

$$F_{ij} = \bar{g}_i^T \underline{G}_j. \tag{15.38}$$

With the help of the chain rule for derivatives, an explicit expression of the inverse of the deformation gradient tensor can be obtained

$$F_{ij}^{-1} = \frac{\partial \alpha_i}{\partial X_j}. \tag{15.39}$$

Introducing the displacement field, eq. (15.32) into eq. (15.36) yields the deformation gradient tensor in terms of the displacement vector components

$$F_{ij} = \delta_{ij} + u_{i,j}. \tag{15.40}$$

15.3.3 The metric tensor

Relationship (15.28b) shows that the metric tensor, G_{ij}, is, in fact, a measure of the deformation. When used as strain measure, the metric tensor is also called the *Green deformation tensor*, or the *Cauchy-Green deformation tensor*. The metric tensor is clearly related to the engineering strain components. Indeed, eq. (15.34) implies

$$\varepsilon_1 = \frac{\|\underline{G}_1 \mathrm{d}\alpha_1\| - \|\bar{g}_1 \mathrm{d}\alpha_1\|}{\|\bar{g}_1 \mathrm{d}\alpha_1\|} = \sqrt{G_{11}} - 1. \tag{15.41}$$

Similar relations hold for ε_2 and ε_3. The angular distortion, eq. (15.35) becomes

$$\gamma_{23} = \arcsin \frac{G_{23}}{\sqrt{G_{22} G_{33}}}. \tag{15.42}$$

The inverse relationships are readily obtained as

$$G_{11} = (1 + \varepsilon_1)^2, \tag{15.43a}$$

$$G_{23} = (1 + \varepsilon_2)(1 + \varepsilon_3) \sin \gamma_{23}. \tag{15.43b}$$

The metric tensor in the deformed configuration is closely related to the deformation gradient tensor. Introducing eq. (15.37) into the definition of the metric tensor, eq. (15.29b), yields

$$G_{ij} = F_{ki} F_{kj}. \tag{15.44}$$

15.3.4 The Green-Lagrange strain tensor

A widely used strain measure is the *Green-Lagrange strain tensor*, defined as

$$e_{ij} = \frac{1}{2}(G_{ij} - g_{ij}). \tag{15.45}$$

It is also called the *Lagrangian strain tensor*, or the *Green-Saint Venant strain tensor*. The Green-Lagrange strain tensor is closely related to the metric tensor, and eqs. (15.43) reveal its connection to the engineering strain components,

$$e_{11} = \frac{1}{2}\,(G_{11} - 1) = \varepsilon_1 + \frac{1}{2}\varepsilon_1^2, \tag{15.46a}$$

$$e_{23} = \frac{1}{2}(G_{23} - 0) = \frac{1}{2}(1 + \varepsilon_2)(1 + \varepsilon_3)\sin\gamma_{23}. \tag{15.46b}$$

If the deformation of the body is such that the strain components remain far smaller than unity, the above relations simplify to

$$e_{11} \approx \varepsilon_1, \quad e_{23} \approx \frac{1}{2}\gamma_{23}. \tag{15.47}$$

The Green-Lagrange strain tensor is closely related to the deformation gradient tensor. Indeed, introducing eq. (15.44) into eq. (15.45) yields

$$e_{ij} = \frac{1}{2}(F_{ki}F_{kj} - g_{ij}). \tag{15.48}$$

The Green-Lagrange strain tensor is also closely related to the change in length of the increment of the position vector. Indeed, eqs. (15.28a) and (15.28b) yield

$$\frac{1}{2}(\mathrm{d}S^2 - \mathrm{d}s^2) = \frac{1}{2}(G_{ij} - g_{ij})\,\mathrm{d}\alpha_i\mathrm{d}\alpha_j = e_{ij}\,\mathrm{d}\alpha_i\mathrm{d}\alpha_j. \tag{15.49}$$

Finally, the Green-Lagrange strain tensor is readily expressed in terms of the displacement components by introducing eq. (15.40) into eq. (15.48) to find

$$e_{ij} = \frac{1}{2}(u_{i,j} + u_{j,i} + u_{k,i}u_{k,j}). \tag{15.50}$$

15.4 Strain measures for various differential elements

The previous section has focused on the state of strain at a point of a three-dimensional solid. It is often useful, however, to characterize the straining of a differential line, surface, or volume element of the body. These issues are addressed in the following sections.

15.4.1 Stretch of a material line

In the reference configuration, the orientation of material line **PQ** is defined by a unit vector, denoted $\bar{n}$, defined as

$$\bar{n} = \frac{\mathbf{PQ}}{\|\mathbf{PQ}\|} = \frac{\mathrm{d}\alpha_i}{\mathrm{d}s}\,\bar{g}_i = n_i\,\bar{g}_i. \tag{15.51}$$

The stretch, λ, of this material line is defined as the ratio of the length of the differential elements in the reference and deformed configurations, given by eqs. (15.28a) and (15.28b), respectively, to find $\lambda^2 = \mathrm{d}S^2/\mathrm{d}s^2 = G_{ij}(\mathrm{d}\alpha_i/\mathrm{d}s)(\mathrm{d}\alpha_j/\mathrm{d}s) = G_{ij}\,n_in_j$. The stretch of the line element is now

$$\lambda = \sqrt{G_{ij}\,n_in_j} = \sqrt{F_{ki}F_{kj}\,n_in_j}. \tag{15.52}$$

15.4.2 Angle between two material lines

Consider two material lines defined by unit vectors $\bar{n}$ and $\bar{n}'$ with stretches λ and λ', respectively. The scalar product of the position increments corresponding to these material lines is $\mathrm{d}\underline{X}^T \mathrm{d}\underline{X}' = \|\mathrm{d}\underline{X}\| \, \|\mathrm{d}\underline{X}'\| \cos\theta$, where θ is the angle between the two material lines in the deformed configuration. Solving for this angle yields $\cos\theta = (\mathrm{d}\underline{X}/\mathrm{d}S)^T (\mathrm{d}\underline{X}'/\mathrm{d}S')$. Using the chain rule for derivatives, and introducing the definition, eq. (15.36), of the deformation gradient tensor yields

$$\cos\theta = F_{ik} F_{il} \frac{\mathrm{d}\alpha_k}{\mathrm{d}s} \frac{\mathrm{d}s}{\mathrm{d}S} \frac{\mathrm{d}\alpha'_l}{\mathrm{d}s'} \frac{\mathrm{d}s'}{\mathrm{d}S'},$$

and finally

$$\cos\theta = \frac{F_{ik} F_{il} \, n_k n'_l}{\lambda\lambda'} = \frac{G_{ij} \, n_i n'_j}{\lambda\lambda'}. \tag{15.53}$$

15.4.3 Surface dilatation

Consider now the area of the rectangle defined by vectors $\bar{g}_2 \, \alpha_2$ and $\bar{g}_3 \, \alpha_3$. The material particles forming that surface before deformation are located in the surface defined by vectors $\underline{G}_2 \, \mathrm{d}\alpha_2$ and $\underline{G}_3 \, \mathrm{d}\alpha_3$ after deformation. The initial area $\mathrm{d}a_1$, is found from fig. 15.8 as

$$\mathrm{d}a_1 = \|\widetilde{g}_2 \, \bar{g}_3 \, \mathrm{d}\alpha_2 \mathrm{d}\alpha_3\| = \mathrm{d}\alpha_2 \mathrm{d}\alpha_3. \tag{15.54}$$

The area in the deformed configuration, $\mathrm{d}A_1$, is similarly found

$$\mathrm{d}A_1 = \|\widetilde{G}_2 \, \underline{G}_3 \mathrm{d}\alpha_2 \mathrm{d}\alpha_3\| = \sqrt{\underline{G}_3^T \widetilde{G}_2^T \, \widetilde{G}_2 \, \underline{G}_3} \, \mathrm{d}\alpha_2 \mathrm{d}\alpha_3 = \sqrt{G_{22} G_{33} - G_{23}^2} \, \mathrm{d}\alpha_2 \mathrm{d}\alpha_3.$$

Clearly, quantity $G_{22} G_{33} - G_{23}^2 = G G_{11}^{-1}$, where G_{ij}^{-1} is the inverse of the metric tensor and G its determinant. Hence,

$$\mathrm{d}A_1 = \sqrt{G G_{11}^{-1}} \, \mathrm{d}a_1, \tag{15.55}$$

where

$$G = \det(G_{ij}). \tag{15.56}$$

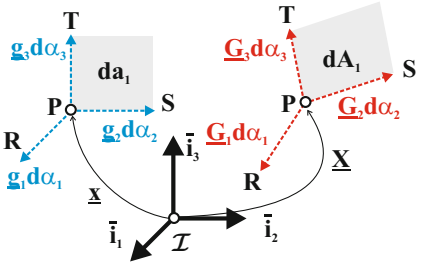

Fig. 15.8. Dilatation of a differential element of area.

Similar developments yield expressions for areas $\mathrm{d}a_2$ and $\mathrm{d}a_3$, and $\mathrm{d}A_2$ and $\mathrm{d}A_3$ for the reference and deformed configurations, respectively. Combining all results then yields

$$\mathrm{d}A_i = \sqrt{G G_{ii}^{-1}} \, \mathrm{d}a_i, \quad \text{no sum on i.} \tag{15.57}$$

The *surface dilatation*, Σ_i, is defined as the relative change in area of a differential element in the deformed and reference configurations and is readily found from eq. (15.57) as

$$\Sigma_i = \frac{\mathrm{d}A_i - \mathrm{d}a_i}{\mathrm{d}a_i} = \sqrt{G G_{ii}^{-1}} - 1, \quad \text{no sum on i.} \tag{15.58}$$

15.4.4 Volume dilatation

Figure 15.7 depicts the volume spanned by vectors $\bar{g}_1\ \mathrm{d}\alpha_1$, $\bar{g}_2\,\mathrm{d}\alpha_2$, and $\bar{g}_3\ \mathrm{d}\alpha_3$. The particles contained in that volume before deformation are located in the volume defined by vectors $\underline{G}_1\ \mathrm{d}\alpha_1$, $\underline{G}_2\ \mathrm{d}\alpha_2$, and $\underline{G}_3\ \mathrm{d}\alpha_3$ after deformation. The volume, $\mathrm{d}v$, in the reference configuration is found from eq. (1.32) as

$$\mathrm{d}v = \bar{g}_1^T \tilde{g}_2\, \bar{g}_3\ \mathrm{d}\alpha_1\mathrm{d}\alpha_2\mathrm{d}\alpha_3 = \mathrm{d}\alpha_1\mathrm{d}\alpha_2\mathrm{d}\alpha_3. \tag{15.59}$$

The volume, $\mathrm{d}V$, in the deformed configuration is

$$\mathrm{d}V = \underline{G}_1^T \widetilde{G}_2\, \underline{G}_3\ \mathrm{d}\alpha_1\mathrm{d}\alpha_2\mathrm{d}\alpha_3 = \det(F_{ij})\ \mathrm{d}\alpha_1\mathrm{d}\alpha_2\mathrm{d}\alpha_3. \tag{15.60}$$

In view of eq. 15.44, $\det(G_{ij}) = \det(F_{ki}F_{kj})$, and hence $\det(F_{ij}) = \sqrt{\det(G_{ij})} = \sqrt{G}$. The *volumetric strain*, or relative change in volume is now defined as

$$\Delta = \frac{\mathrm{d}V - \mathrm{d}v}{\mathrm{d}v} = \sqrt{G} - 1. \tag{15.61}$$

15.4.5 Problems

Problem 15.1. Deformed elastic body

Figure 15.9 depicts an elastic body in its reference and deformed configurations. The displacement field is given as $u_1 = \alpha_1\alpha_2/4$ and $u_2 = -\alpha_1\alpha_2/8$. *(1)* Evaluate the base vectors in the reference and deformed configurations. *(2)* Find the deformation gradient tensor. *(3)* Determine the metric tensors in the reference and deformed configurations. *(4)* Evaluate the Green-Lagrange strain tensor, and *(5)* the physical strain components. Consider point **A** (located at $\alpha_1 = \alpha_2 = 1$) and two material lines $\bar{n}_1$ and $\bar{n}_2$ parallel to $\bar{i}_1$ and $\bar{i}_2$, respectively. *(1)* Find the stretch of the material lines $\bar{n}_1$ and $\bar{n}_2$. *(2)* Determine the angle between the two material lines in the deformed configuration, *(3)* the surface dilatation, Σ_3, at point **A**, and *(4)* the volumetric strain, Δ, at point **A**.

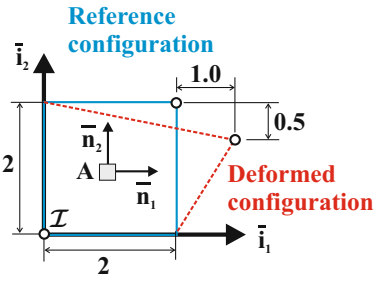

Fig. 15.9. Configuration of the elastic body.

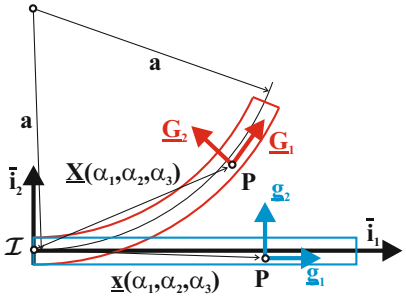

Fig. 15.10. Configuration of the cantilevered beam.

Problem 15.2. Deformed cantilevered beam
Figure 15.10 shows a cantilevered beam of length a and depth h in its reference and deformed configurations. The position vector in the reference configuration is $\underline{x} = \alpha_1\,\bar{\imath}_1 + \alpha_2\,\bar{\imath}_2 + \alpha_3\,\bar{\imath}_3$, and in the deformed configuration

$$\underline{X} = \left\{(a-\alpha_2)\sin\left[(1+\Delta)\,\frac{\alpha_1}{a}\right]\right\}\bar{\imath}_1 + \left\{a-(a-\alpha_2)\cos\left[(1+\Delta)\,\frac{\alpha_1}{a}\right]\right\}\bar{\imath}_2 + \alpha_3\,\bar{\imath}_3,$$

where Δ is a strain measure. *(1)* Find the base vectors in the reference and deformed configurations. *(2)* Determine the deformation gradient tensor, *(3)* the metric tensor, *(4)* the Green-Lagrange strain tensor, *(5)* the physical strain components, and *(6)* the volume dilatation at points **A** (located at $\alpha_1 = a/2, \alpha_2 = h/2, \alpha_3 = 0$) and **B** (located at $\alpha_1 = a/2, \alpha_2 = -h/2, \alpha_3 = 0$). *(7)* Evaluate the surface dilatations Σ_1, Σ_2, and Σ_3 at points **A** and **B**.

15.5 The formulation of small strain problems

At the heart of the formulation of problems involving small strain is the decomposition of the deformation gradient tensor into rigid body motion and deformation. In section 15.5.1, the decomposition of the deformation gradient tensor is described. This leads to a modified principle of virtual work. The implications of the small strain assumption are then discussed in detail in section 15.5.2.

15.5.1 Decomposition of the deformation gradient tensor

Fig. 15.11 depicts the base vectors at a material point of a deformable body in the reference and deformed configurations. The analysis of the metric tensor presented in section 15.3.3 demonstrates that the base vectors in the deformed configuration do not form an orthogonal basis. Indeed, eqs. (15.43) show that these base vectors are not unit vectors, nor are they mutually orthogonal.

Consider an orthonormal basis of arbitrary orientation denoted $\mathcal{J} = (\bar{\jmath}_1, \bar{\jmath}_2, \bar{\jmath}_3)$. The position vector of a material point in the deformed configuration is now resolved in this basis as

$$\underline{X} = X_i^*\,\bar{\jmath}_i. \tag{15.62}$$

The base vectors in the deformed configuration then become

$$\underline{G}_i = \frac{\partial \underline{X}}{\partial \alpha_i} = \frac{\partial X_j^*}{\partial \alpha_i}\,\bar{\jmath}_j = \hat{F}_{ji}\,\bar{\jmath}_j, \tag{15.63}$$

where the following modified deformation gradient tensor was defined

$$\hat{F}_{ij} = \frac{\partial X_i^*}{\partial \alpha_j}. \tag{15.64}$$

A scalar product of eq. (15.63) by $\bar{\jmath}_l$ yields an alternative definition of this tensor

$$\hat{F}_{ij} = \bar{\jmath}_i^T\,\underline{G}_j. \tag{15.65}$$

The two deformation gradient tensors defined in eqs. (15.38) and (15.65) can be related by equating the two expressions for the base vectors in the deformed configuration, eqs. (15.37) and (15.63), to find $\underline{G}_i = \hat{F}_{ji}\,\bar{\jmath}_j = F_{ji}\,\bar{g}_j$. A scalar product of this result by $\bar{g}_l$ yields the desired relationship, $F_{ij} = (\bar{g}_i^T \bar{\jmath}_k)\,\hat{F}_{kj}$. Because the base vectors in the reference configuration form the orthonormal basis $\mathcal{I}$, see eq. (15.26), rotation tensor $\underline{\underline{R}}$ brings basis $\mathcal{I}$ to basis $\mathcal{J}$, and $R_{ij} = \bar{g}_i^T \bar{\jmath}_j$. The relationship between the two deformation gradient tensors now simply becomes

$$F_{ij} = R_{ik}\hat{F}_{kj}. \tag{15.66}$$

This decomposition expresses the deformation gradient tensor as the product of rotation tensor $\underline{\underline{R}}$, defining a rigid body rotation, by deformation gradient tensor $\underline{\underline{\hat{F}}}$, defining the deformation of the body at that point.

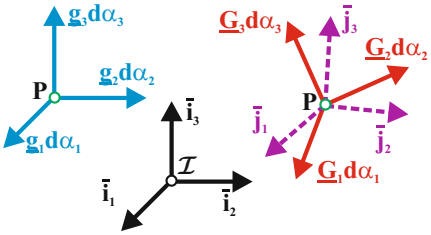

Fig. 15.11. The base vectors in the reference and deformed configurations.

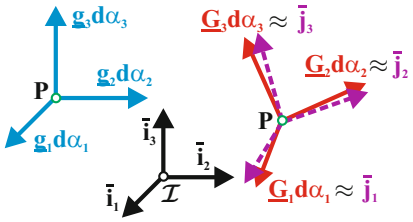

Fig. 15.12. Deformation of a differential element.

15.5.2 The small strain assumption

Consider the deformation of a differential element of the body depicted in fig. 15.12. The norm of base vector $\underline{G}_1$ in the deformed configuration was found in eq. (15.43a) to be closely related to the engineering strain component, ε_1,

$$\|\underline{G}_1\|^2 = G_{11} = (1+\varepsilon_1)^2 = 1 + 2\varepsilon_1 + \varepsilon_1^2. \tag{15.67}$$

Similarly, the angular distortion between $\underline{G}_2$ and $\underline{G}_3$ is closely related to the engineering strain component, γ_{23}, see eq. (15.43b),

$$\frac{\underline{G}_2^T \underline{G}_3}{\|\underline{G}_2\|\|\underline{G}_3\|} = \sin\gamma_{23}. \tag{15.68}$$

In numerous applications, thin structures such as cables, membranes, beam, plates, and shells undergo finite displacements and rotations while strain components remain very small. The small strain assumption states that *relative elongations and angular distortions are negligible compared to unity, i.e.*,

$$|\varepsilon_1|, |\varepsilon_2|, |\varepsilon_3| \ll 1, \quad |\gamma_{23}|, |\gamma_{13}|, |\gamma_{12}| \ll 1. \tag{15.69}$$

Introducing this approximation in eq. (15.67) and (15.68) yields

$$\|\underline{G}_1\|^2 = G_{11} \approx 1, \quad \frac{\underline{G}_2^T \underline{G}_3}{\|\underline{G}_2\| \|\underline{G}_3\|} \approx 0.$$

In other words, the base vectors in the deformed configuration approximately define an orthonormal basis because each base vector is approximately of unit length, and they are nearly orthogonal to each other. For small strain problems, orthonormal basis $\mathcal{J}$ defined in section 15.5.1 will be selected to be nearly coincident with the base vectors in the deformed configuration, *i.e.*,

$$\underline{G}_i \approx \bar{\jmath}_i. \tag{15.70}$$

Consequently, basis $\mathcal{J}$ is called the *convected* or *material* frame. Introducing this approximation in eq. (15.63) leads to $\underline{G}_i = \hat{F}_{ji}\, \bar{\jmath}_j \approx \bar{\jmath}_i$. A scalar product of this result by $\bar{\jmath}_p$ then yields $\hat{F}_{ij} \approx \delta_{ij}$. Finally, using eq. (15.66)

$$F_{ij} \approx R_{ij}. \tag{15.71}$$

In other words, when the strain components are very small, the deformation gradient tensor is approximately equal to the finite rotation tensor that brings basis $\mathcal{I}$ to $\mathcal{J}$.

Under the assumption of small strains, it can be shown that the principle of virtual work becomes

$$\int_{t_i}^{t_f} \int_{\mathcal{V}} \left[\tau^{*ij} \delta\gamma_{ij} - \underline{p}^T \delta\underline{v}\right] \, \mathrm{d}\mathcal{V}\mathrm{d}t = \int_{t_i}^{t_f} \left\{ \int_{\mathcal{V}} \underline{b}^T \delta\underline{u} \, \mathrm{d}\mathcal{V} + \int_{\mathcal{S}} \hat{\underline{t}}^T \delta\underline{u} \, \mathrm{d}S \right\} \mathrm{d}t - \left[\int_{\mathcal{V}} \hat{\underline{p}}^T \delta\underline{u} \, \mathrm{d}\mathcal{V} \right]_{t_i}^{t_f}. \tag{15.72}$$

In this principle, the strain measures are defined as

$$\gamma_{ij} = \frac{1}{2}(\hat{F}_{ij} + \hat{F}_{ji}) - \delta_{ij}, \tag{15.73}$$

and the stress measures, τ^{*ij}, form the convected Cauchy stress tensor, *i.e.*, the components of the true stress tensor in basis $\mathcal{J}$. This statement of the principle of virtual work will be used in subsequent sections to derive the governing equations of structures undergoing large displacements and rotations but small strains.